HEALTH SYSTEMS
2025, VOL. 14, NO. 1, 12–30
https://doi.org/10.1080/20476965.2023.2287506

RESEARCH ARTICLE

OPEN ACCESS Check for updates

Application of a composite, multi-scale COVID-19 mitigation framework: US border use-case

Zach Danial, Nathan Edwards, John James, Paula Mahoney, Casey Corrado and Brian Savage

The MITRE Coporation, Tysons, VA, USA

ABSTRACT

Airborne pathogen transmission within crowded facilities can be modelled by combining several interrelated mechanisms of spread: movement of people, airflow dynamics, and aerosol dispersion. This paper describes a composite model framework combining analytical models to demonstrate the spread of an airborne pathogen in a crowded, confined space at an immigrant processing centre on the southern US border during the border crisis of March 2021. Recommendations that could reduce current COVID-19 infection rate from 11% to 6.16% at relatively low additional cost to the government are given. These recommendations could also lower the infection rate by approximately five times from 31.14% worst case from long indoor exposures down to 6.35% when immigrant processing times surge to 10 days. This work highlights the challenges of managing COVID-19 in crowded facilities, and provides quantitative decision options with potential both to slow and prevent disease spread, while lessening the economic burden on communities.

ARTICLE HISTORY
Received 13 April 2022
Accepted 13 November 2023

KEYWORDS
Modeling and simulation; composite hybrid model; multiscale; multi-paradigm; disease mitigation; COVID-19

1. Introduction

Motivated by the developments on the US southern border in early 2021 (Kanno-Youngs, 2021), modelling and simulation efforts were used to understand the impact of changes in migration patterns on the course of the COVID-19 (SARS-CoV-2) pandemic within the continental United States and to help define cost-effective strategies to minimise the resulting disease spread. Reducing airborne SARS-CoV-2, particularly indoors, remains the leading strategy to prevent COVID-19 among the unvaccinated (Chagla et al., 2020). A primary motivator of this effort was the recognition that the ability to model the spread of an airborne pathogen at multiple scales was necessary for the specific use-case, yet no known model existed for this purpose.

In this paper, we describe and demonstrate the application of a novel composite multi-scale, multi-paradigm model framework which combines the analytical domains of airborne transmission, fluid dynamics, and movement of people with agent-based modelling to demonstrate the spread of an airborne pathogen in a crowded indoor environment. While many of the computational interaction details of each model domain have been abstracted for the purpose of describing the foundational framework, our key contributions to the scientific community are centred around how to establish such a composite (or hybrid) model in the healthcare domain along with describing the challenges, considerations, and nuances of the multi-scale, multi-paradigm approach when combined with a SEIR compartmental epidemiological model and societal cost model as decision aids for infectious disease mitigation. We also demonstrate the framework's utility by applying it to a crowded US border processing facility during a peak time in the COVID-19 pandemic.

1.1. Literature review

There have been many papers published since the start of the COVID-19 pandemic aimed at guiding decision-makers to the proper non-pharmaceutical interventions (NPIs). Some early work focuses on large-scale transmission (countries) (Cuevas, 2020; De Visscher, 2020; Timothy et al., 2020), which is still informative but does not yield specific guidance for decision-makers. Other research has been focused on decision-making at the scale of a single institution (Cuevas, 2020; Wildman et al., 2020; Zhou et al., 2021), but do not take into account the combined effect of NPIs associated with mask effectiveness, airflow, and ventilation, all of which have proven to be very successful in preventing significant COVID-19 transmission during air travel (Bhuvan et al., 2021) and on buses (Benjamin & Zimmerman, 2021; Ramirez et al., 2021).

Two agent-based models to highlight are The Artificial University (TAU) and COVASIM. TAU was developed as a configurable, open-source computer simulation that utilises a contact network based on

CONTACT Zach Danial zdanial@mitre.org The MITRE Coporation, Tysons, VA 7596

real-world information about university activities and interactions (Wildman et al., 2020). This study evaluated the effectiveness of various interventions and testing protocols on health outcomes within an artificial university setting of 6,500 individuals. The results indicated that physical distancing and centralised contact tracing were the most effective at reducing infections, although there was a compliance threshold below which physical distancing was less effective.

COVASIM is an agent-based simulation of COVID-19 spread that allows researchers and decision makers to test the effect of a number of disease spread interventions (Kerr et al., 2021). It accounts for location-specific demographics with a heterogeneous transmission network. Agents can belong to entities/institutions that produce the contact networks, including households, schools, workplaces, long-term care facilities, and communities. The model features age-specific outcomes from infection, as well as transmission dynamics within an agent due to the time evolution of viral load. In order to reduce the computational intensity of the agent-based approach, COVASIM dynamically rescales the population represented by a single "agent" as the infectious population grows.

Several studies have demonstrated the utility of hybrid agent-based (ABM)-compartmental models and hybrid computational fluid dynamics (CFD)-exposure risk models in simulating the spread of COVID-19 and the effectiveness of interventions. Researchers have used a hybrid approach combining ABMs with compartmental models to reduce computational intensity while maintaining model fidelity. Hunter et al. (2020) uses a hybrid compartmental and agent-based approach to reduce the computational intensity of simulating disease spread among large populations. The model implementation transitions between the agent-based and equation-based architectures when the population of infected agents crosses certain thresholds. The authors found that computational time is significantly reduced without losing fidelity. The following papers also benefit from speed up of hybrid approach, and target model granularity towards a focused set of interventions. Chen et al. (2021) implements a hybrid model combining mean-field (SEIR; Susceptible, Exposed, Infectious, Recovered) and agent-based approaches to study the effects of interventions targeted towards health-care workers on the spread of Ebola in Sierra Leone. While the researchers use a mean-field approach for modelling the population at large, the compartmental model is coupled to an agent-based model of health-care workers who can participate in interventions including pre-deployment training and vaccination. Similarly, Nguyen et al. (2022) uses a hybrid compartmental and agent-based model, but with the ABM granularity targeted towards the sharing of health-care and administrative staff among care homes. The model implements a temporary staff module and intra-facility module to study how staff sharing across care homes can lead to disease spread and outbreaks within and across a network of facilities. The researchers opted for a stochastic SEIR to capture the range of outcomes (outbreaks and zero-cases), and the associated risk of these outcomes.

In addition to ABM-compartmental models, researchers have also used hybrid CFD and exposure risk models to study the transmission of COVID-19. Ramajo et al. (2022) uses a hybrid Euler/Lagrange CFD to simulate the effect of rooftop HVAC (Heating, Ventilation, and Air-Conditioning) on COVID-19 transmission risk on urban buses, and the Wells-Riley risk model to calculate the associated infection risk. The model uses Lagrangian approach (particle/trajectory based) to model transmission from sneezing and coughing, and the Eulerian (continuous/field based) approach for modelling transmission from breathing and talking. While results show that centralised rooftop HVAC reduces the concentration of infectious particles in the central zone of the bus, it is not sufficient for the front and the sides of the vehicle. However, the average Wells-Riley risk across the vehicle can be reduced by more than 50% with 10 air changes per hour (ACH). Related research, (Drossionos, 2022) describe that a current research challenge is to incorporate microenvironmental models, virus transmissibility and infectivity into epidemiological models (e.g., SEIR) at mesoscale and to calculate the health risk.

In conclusion, the utility of both ABM-compartmental models and hybrid CFD-exposure risk models has been demonstrated in several studies for simulating the spread of COVID-19 and the effectiveness of interventions. Our approach uses a hybrid of CFD, exposure risk, ABM, and compartmental models to allow high-fidelity intervention modelling, an agent-based/compartmental boundary (facility vs city) to show the second-order effects of interventions at the facility.

1.2. Our approach

Airborne pathogens utilise several transportation mechanisms to spread locally and across larger geographies. Aerosol dispersion (e.g., from talking, singing, or coughing) accounts for transmission within close proximity; airflow patterns within a confined space can contribute to spreading these aerosols further; and migration of people carries the entire viral load to even more disparate destinations. Driven by these mechanisms of spread, we developed a composite model of airborne pathogen transmission within crowded facilities by combining four interrelated models to holistically estimate the spread and risk of the airborne pathogen: computational fluid

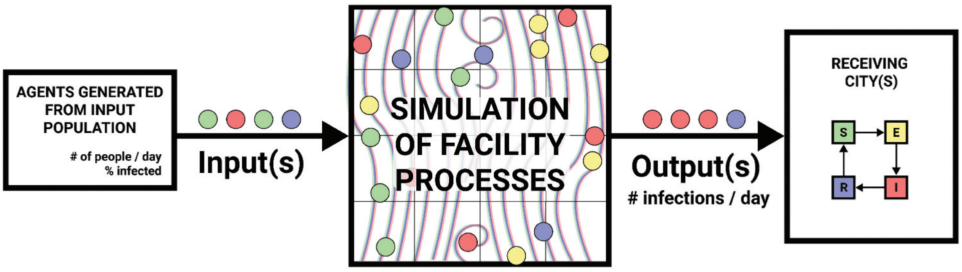

Figure 1. Composite model in its most general form.

dynamics (CFD) for movement of air through the facility, an analytical Aerosol Risk (AR) model for airborne transmission, an agent-based model (ABM) to account for the interactions of people within the facility and a compartmental system dynamics model (SEIR) to measure pathogen spread from immigration facilities into local communities and across cities and states, nationwide. The outcome of the composite model is a comparison of costs to society (SC) to also aid in mitigation decision-making.

We parameterise the model to quantify the benefits of certain NPIs to their associated costs and implementation challenges. Examples of this include, but are not limited to, changing the time people are in the facility, air-return and air-register placement, sizing of the HVAC system, and mask-wearing compliance. Benefits are measured against total impact of the pathogen on people within the facility upon release, and the impact of surrounding communities as the pathogen is spread by people leaving the facility.

This paper is divided into three additional sections. Section 2 dives into the methodology of composing such as model while considering multi-scale and multi-domain modelling complexities and provides a generalised description of the composite model, specific aspects of each individual model, and how each of the individual models fit into the whole. Section 3 describes the application of the model to our motivating use-case: immigrants arriving and dispositioned at a processing centre on the US southern border. And finally, Section 4 describes the theoretical basis of our applied methods, model validation, and offers discussion and conclusions.

2. Methodology of model composition

Composing a multiscale and multi-paradigm model comes with complexities related to integrating multiple systems with paradigms of different underlying dynamics. Prior research categorises the current body of work as a transdisciplinary hybrid model that is characterised by systematic integration of constructs from different scientific disciplines (Tolk et al., 2021) and is associated with “wicked problems”. The key challenge is on the composability of such a hybrid model which is still an open research question.

The focus of this work is on the composition of a multiscale, multi-paradigm model rather than the intricate details of each sub-model used. Subsequently, this section presents basic descriptions of each model so that the composition theory and methodology can be discussed in Section 4.1. In the model’s most general form, there are three domains and prescribed flows among them (Figure 1) followed by a feedback path where the facility state and output flow may affect upstream region(s).

- Upstream: Agents created with upstream attributes (i.e., demographics, susceptibility, and metadata) enter the facility daily.
- Facility: Agents interact with each other and the environment according to prescribed process model (interaction network structure, facility operations). Agents are susceptible to aerosol contaminant.
- Downstream: Agents leave facility with modified attributes and assimilate in the receiving city(s).

The composite model (Figure 2) leverages CFD simulations of facility geometry and HVAC system to calculate the effect of physical barriers to airflow within the facility/facilities (e.g., partitions, classrooms, hospital rooms and wings, offices, and conference rooms). The resulting airflow and ventilation characteristics are then used as inputs to the AR model to calculate a transmission risk factor based on viral emissions and mitigations (airflow, mask effectiveness, and population density) as they relate to close contacts. The ABM uses the aerosol risk factor to allocate infectious aerosol attacks to agents based on where they are located and who they encounter. In the case of a highly transmissible virus, the interaction network between people plays a critical role in determining disease spread. The ABM outputs the number of infected individuals leaving the facility to the downstream region(s) daily; in the SEIR model, the contagious agents mix in the downstream region(s), contributing to cases, hospitalisations, and deaths. Societal costs are then calculated based on the valuation of statistical life and average cost of a COVID-19 hospitalisation (Hackett, 2020; U.S. Department of Transportation, 2021).

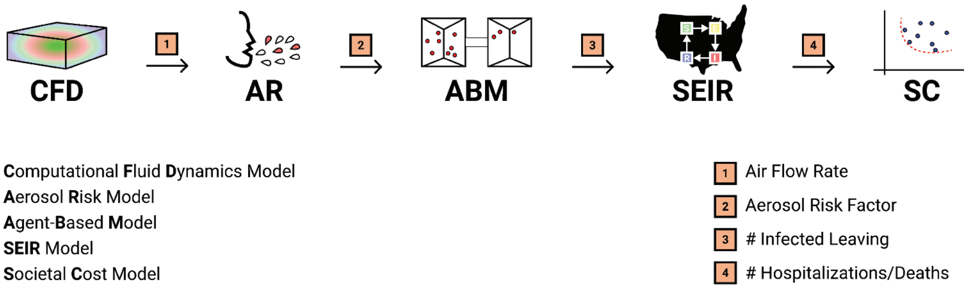

Figure 2. Airborne disease transmission model composition pipeline.

Control variables are parameterised NPIs (ventilation, changes to facility geometry, facility process/operations, masking), which alter the values of key scenario attributes. We use the simulation to explore the decision space to optimise mitigation strategy with respect to upfront costs and downstream impact.

A *scenario* encodes the upstream flow into the facility (with population magnitude and metadata, such as demographic information), facilities geometry, agent interaction network, and the flow leaving the facility (magnitude and metadata). By properly modelling the respective scenarios considering the agent-based network structures and classes of agents, the framework described herein can also be applied to schools, hospitals, workplaces, in addition to the current use-case focused on the US border facilities.

2.1. Computational fluid dynamics model

CFD uses numerical methods to simulate the fluid flow within a space, providing results on flow rate, particle trajectory, etc. In this case, CFD modelling was used to evaluate the airflow within the building in question, identifying potential areas of concern (low airflow) where COVID-19 transmission could be high. In addition, this analysis investigated how opening or closing the doors to the portioned rooms would affect airflow: an increase of the overall airflow rate to these spaces therefore decreases the risk of COVID-19 transmission (Parhizkar et al., 2022). The results of this analysis can be used to inform both short-term changes to facilities and design decisions for new buildings. To complete a CFD simulation, a computer aided design (CAD) model of the building and specifications about the airflow within that space are required. A CAD model was developed using Ansys 2021R1 to represent this space, and HVAC specifications provided by the facility were used to produce a fluid flow analysis. The CFD airflow rates and resulting air changes per hour (ACH) assist in the aerosol risk quantisation, however the airflow dynamics as shown in the CFD streamlines (see Figure 8 in Section 3) help gain significant understanding of infectious aerosol travel or accumulation in stagnant regions. More details of the CFD model are described in Appendix A.1.

2.2. Aerosol risk model

An aerosol risk model provides an estimate risk of exposure to airborne contagions or hazards (Mittal et al., 2020; Riley et al., 1978; Rudnick & Milton, 2003; Sze to et al., 2008). In the context of COVID-19 transmission, the model focuses on aerosols that are commonly defined as airborne particles that are 5 μm or less in size and are affected more by airflow and fluid dynamics than deposition from gravity (Pan et al., 2019). Since airborne infectious disease transmission is dependent on the loading human infectious dose (HID) into the respiratory tract, a measured quantity of contagions, and the exposure also strongly depends on nearby concentration(s) of the contagion, respiratory rates of the susceptible person, and the generation source of the contagion. This aerosol risk model primarily focuses on the movement and spread of the contagion through the air and includes effects from air exchange and exposure regions based on infectious aerosol emitters and susceptible people. A broadly used aerosol risk model, Riley et al. (1978) (Riley et al., 1978), and many of the derivative models account for the major factors; however, they primarily consider a well-mixed environment and do not account the fluid dynamics near an infected or susceptible person. The aerosol risk model introduced in this work, built with GNU Octave version 6.2.0, uses the Wells-Riley model as a basis but adds the fluid dynamics and accounts for the aerosol dispersion pattern close to an infectious source, in the nearby vicinity or same room, the effects of wearing face masks or applying air filtration, and is derived from empirical observations of prior aerosol dispersion experimentation (Edwards et al., 2020, 2021).

Close contact of susceptible people to infected is defined by regions of higher infectious aerosol concentration after a dispersion event such as talking, coughing, or sneezing. In many cases, close contact is within a one-metre distance from an infected person (Figure 3) based on our empirical experimentation on

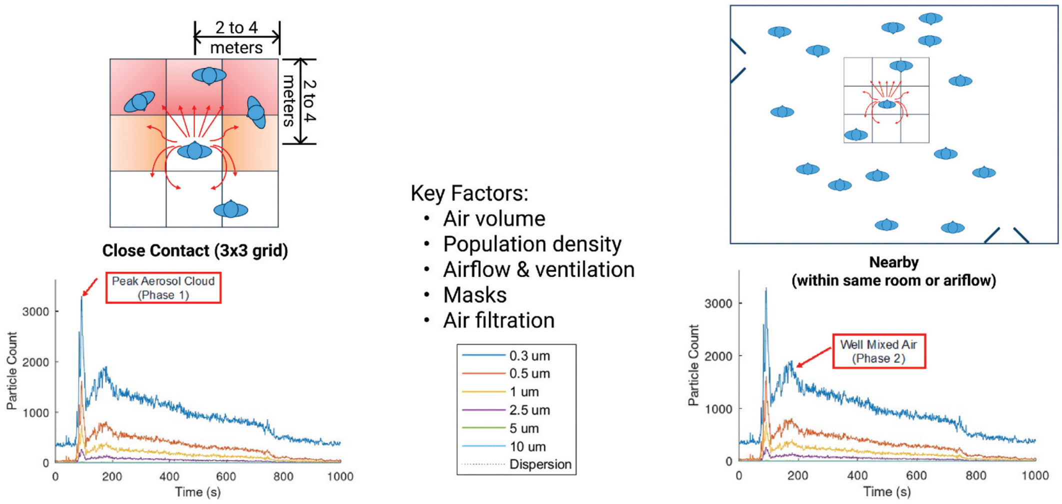

Figure 3. Aerosol model for close contact and nearby (Edwards, n.d.).

aerosol dispersion (Edwards et al., 2020, 2021) and is informed by the air velocity analysis from CFD simulation. In other conditions with poor airflow, the peak concentration aerosol cloud can rapidly spread to 4 metres or more. Viral emissions or inhalation is reduced by the mask efficiency, although mask wearing compliance is not modelled in the aerosol risk model. The viral emissions increase with more infected people in the area. The AR model is run with [t] = [minutes] to calibrate the model, however, the data is presented in days.

Infectious aerosol risk factor $\frac{R_S}{R_B}$, where R_S is the AR risk factor of the scenario and R_B be the AR risk factor of the baseline case. This ratio is used as a relative risk multiplier of the basic infection reproduction number, R_0, and scales the rate of infection in the ABM. Details on the use and interaction between AR and ABM using the risk multiplier are further described in Section 4.1 on the theory. More details of the aerosol risk model are described in Appendix A.2.

2.3. Agent-based infection model

Agent-based modelling focuses on the individual components of a system as opposed to the homogeneous groups of compartmental models. We define behaviour for the components (agents) but study the emergent dynamics of the system. The flexibility of agent-based modelling allows us to implement facility operations to an arbitrary level of detail and simulate the infection process within the facility.

This flexibility allows for the modelling of operational changes without having to change the underlying architecture of the model. This can be particularly useful in the context of a rapidly evolving situation like the COVID-19 pandemic, where new interventions and changes to operating procedures may be implemented frequently. With an agent-based model, it is possible to easily incorporate these changes into the simulation, providing a more accurate representation of the system and allowing for the evaluation of the potential impact of the changes. In our implementation and use case, the processing of different classes of agents through a multistage process is much preferred due to the significant compartment populations and homogenous assumptions necessary in a System Dynamics/SEIR modelling approach.

The agent-based model discussed here-in is a combination of an infection model and the model of the US southern border migration process (discussed in Section 3) implemented in AnyLogic version 8.6. Agents in the model represent individuals, each of which can be in one of six disease states (laid out in Figure 4): susceptible, incubating, infectious (either asymptomatic or symptomatic), recovered, dead, or immune and simultaneously 10 location states: At border, Holding[agent-type], Mexico, Health and Human Services (HHS), Immigration and Customs Enforcement (ICE), Non-Governmental Organisations (NGO), and within the US. The model tracks the movement of these agents through different areas of the facility (see process model in Figure 4) and simulates the spread of the disease as infected agents come into contact with others. The rate of infection is determined by several factors, including the transmissibility of the disease, the presence and effectiveness of masks, the vaccination status of the agents and the number of infected agents in a given agent's location.

The ABM outputs the number of new infections over time, which becomes an input into SEIR. Compartmental epidemic models are the mean field approximations of their agent-based equivalents under the assumption of homogeneity (Kunwar et al., 2021). More details of the ABM model are described in Appendix A.3.

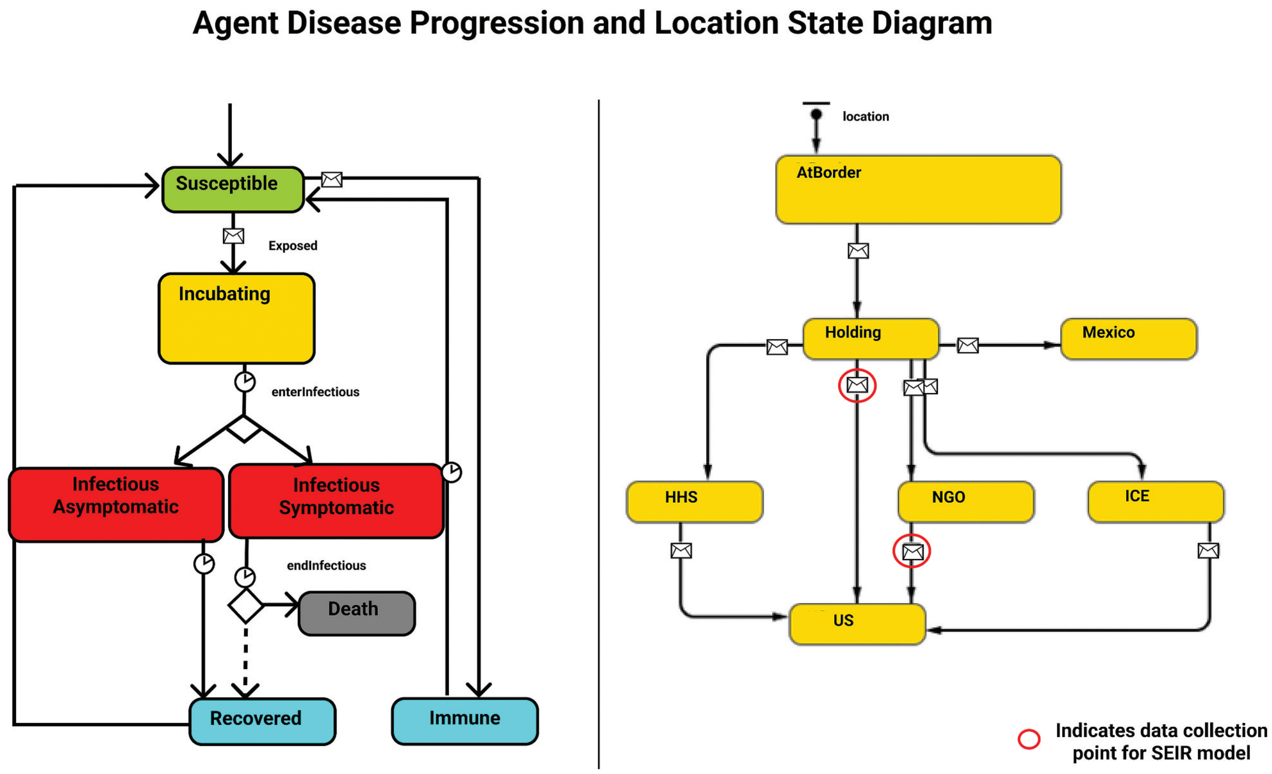

Figure 4. ABM agent disease-progression and location state-diagram implemented in AnyLogic. Counts of infected agents are retrieved at the indicated boxes as infected agents are transferred to the US. Only agents that come directly from Holding or from the NGO are included, as others are assumed not to be released into US population.

2.4. SEIR-Based infection model

Compartmental models such as Susceptible–Infected–Recovered (SIR) models have long been used in epidemiology to understand the high-level system dynamics of disease transmission within a population (Kendall, 1956; Kermack & McKendrick, 1927; Ross, 1916). SIR models can be fit to data and used to gauge the magnitude and timescale of the epidemic, as well as understand the consequences of control decisions (Yarsky, 2021; Young et al., 2021). The system dynamics transmission model (SEIR) used in this body of work was derived from (Aron & Schwartz, 1984) and built on a SEIR framework which accounts for the long incubation period observed during the onset of COVID-19 with potential exposures (E) of susceptible people (The MITRE Corporation, 2020). The SEIR-based infection model used in this work (diagram in Figure 5) combines state and local NPIs, behavioural data, public/private health infrastructure, and empirical findings for the risk of hospitalisation and death, to produce a high-fidelity reconstruction of the epidemic. It contains sub-models for vaccination (according to a prescribed schedule), waning immunity/reinfection, and the rise of new variants. The core of our SEIR implementation is a data structure arrayed by age groups, with each age group having corresponding values for population size, likelihood of hospitalisation, likelihood of becoming critical, and likelihood of death. Additionally, the incubating, infectious, and recovered compartments are also arrayed by virus strain, with a disease severity for each strain. Infection risk is broken down into co-habitant versus social infectivity. The model also includes a blood plasma donation and administration module, as well as a vaccine production and administration module. For each city or metropolitan area, the model includes data on population size, the number of initial infections, the number of hospital beds and ICU beds per 1,000 people, and the number of ventilators per 10,000 people. The model was built using Stella Architect v2.1.3, and uses the included optimisation suite to fit disease severity to reported deaths for the respective location. The SEIR model simulates the pandemic trajectory in cities, metropolitan statistical areas (MSAs), subject to the flow of infected immigrants. More details of the SEIR model are described in Appendix A.4.

2.5. Societal cost model

From the composite model outputs, we then calculate the additional hospitalisations and deaths from the increased number of infections. For purposes of comparison, the excess hospitalisations and deaths are quantified according to FAIR Health's analysis (Hackett, 2020) ∼ $65,000 per COVID-19 hospitalisation and US Department of Transportation using ~ $10,000,000 as the statistical value of life (U.S. Department of Transportation, 2021). We use these costs to represent an NPI portfolio as (investment cost, societal cost/savings) to provide a quantitative decision trade-space on which NPIs should be implemented on-site. More details of the societal cost model are described in Appendix A.5.

The modelling requires that individual immigrant's health, the parameters of the facilities (e.g., HVAC system specifications and dimensions of the rooms), and the duration of the disposition process be taken into account. For each of these three demographics, we attempt to model these parameters as close to reality as possible using our understanding of current policies, and interviews with subject matter experts familiar with the disposition process.

3. Use-case and results: US southern border immigrant processing facility March–April 2021

The composite model was applied to airborne pathogen transmission within the processes and facilities for immigrants who cross the southern border between ports of entry. To aid decision-making and investment, the model compares the benefits of certain NPIs to their associated costs and implementation challenges. We parameterised the model based on a Central Processing Center (CPC) on the US Southern Border c. March-April 2021.

During March–April of 2021, government policies generally led to the following disposition of immigrants (Russonello, 2021): Single Adults (SAs) were returned to Mexico under USC Title 42, members of family units (FMUAs) were provided an asylum date and then released in coordination with non-governmental organisations (NGO), and unaccompanied children (UACs) were processed and transferred to Health and Human Services (HHS). Statistics released publicly by Customs and Border Patrol (CBP), and immigration policies in place at this time, support parameterising the model in this way.

3.1. CBP processing and disposition (CPC) scenario model

The process model of US southern border migration is a body of qualitative information gathered from subject matter experts (SMEs) and US Border Patrol officers. This information includes encounters, booking and disposition processes, facility operations, and local NGO assistance to immigrants after release. Simulated agents in the ABM are created based on arrival rate specific to each demographic. The unaccompanied children are separated into one set of partitions and families into different partitions. Unaccompanied adults are removed from the simulation as they are sent back to Mexico. Children are released to HHS after being processed. The families are released to either NGO or directly to US cities. We implemented the agent-based infection model within the context of the migration process model (Figure 7) to study the effects of NPIs on infection within the facility shown in Figure 6. The ABM calculates the number of infections that happen during this process based

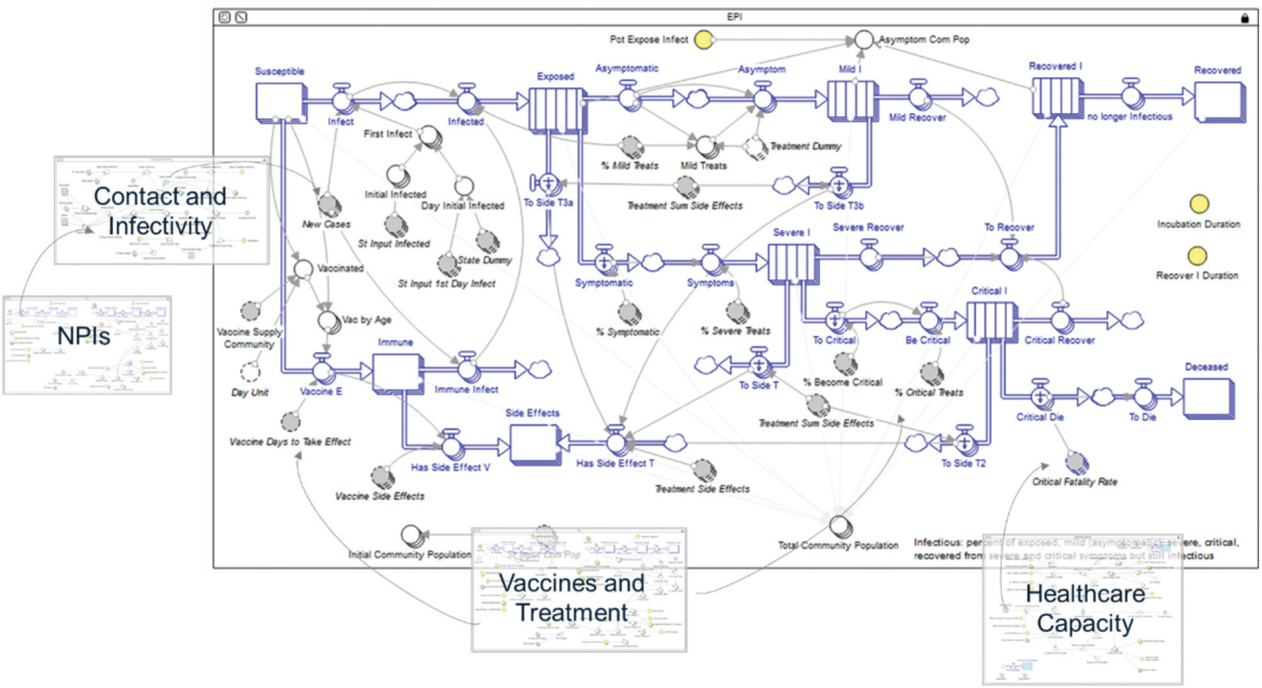

Figure 5. A graphical depiction of the system dynamics logic of the SEIR-based model built in Stella Architect v2.1.3.

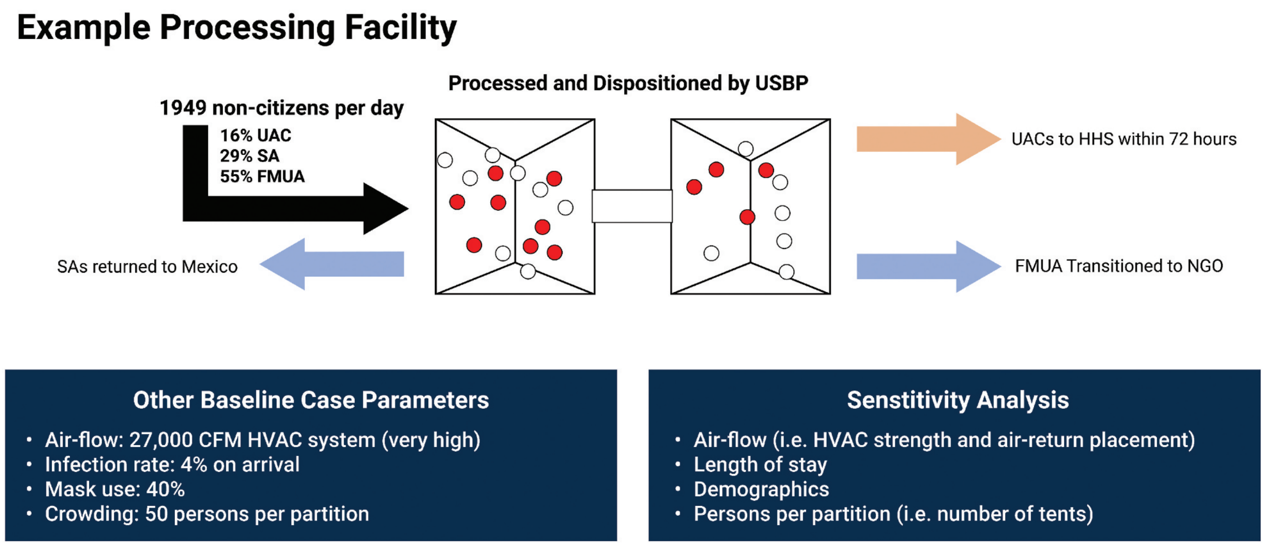

Figure 6. High-level description of flows in and out of the facility and the parameters for the baseline case.

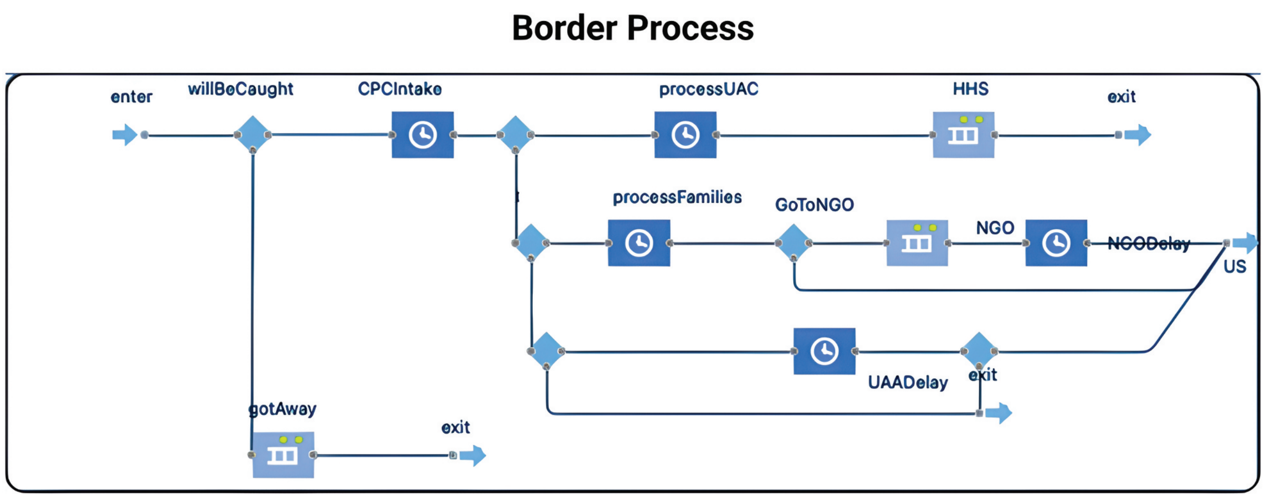

Figure 7. Figure shows the processes modeled at the border facility that involve time. Boxes with clocks are assumed to take constant time. Diamonds are decision points based on type of agent. "GoToNGO" is based on a probability.

on the number of tents, capacity of tent partitions, and immigrant processing time.

Use-Case Inputs

- Arrival rate of encounters
- Percent of each demographic represented in arrivals
- Facility design
- Number of people per partition
- HVAC and resultant airflow dynamics
- Probability that family stays with NGO on release

Outputs

- Steady state values of each demographic in the processing facility.

Key Assumptions Given the immigrant arrival rate and the population size of each immigrant demographic, we adjusted each demographic's length of stay so that the model projected the correct steady state values.

Important Notes The southern border conditions are dynamic, and in some cases, not well understood. Operational changes constantly need to be remodelled to better represent real-world processing. Our model parameterises these less certain characteristics so that more accurate results can easily be obtained by rerunning the model. Even with some uncertainty, the accuracy captured in the parametrisation of the model is sufficient to yield actionable results and still aid in subsequent strategy decisions.

3.2. Parameter and control space

In this section, we discuss features and assumptions of the use-case scenario. More specifically, we describe the accuracy of assumptions in component models specific to the application of this model to the immigrant processing facility and the parameter values used to produce the results of this paper.

3.2.1. Data and qualitative analysis

The data used to put together this composite model was primarily qualitative or recorded/shared one time. The only real-time dataset was COVID-19 deaths, which was used to fit the MSAs.

The baseline infection rate ($\rho = 0.07$) used in the ABM was calculated based on data from CBP, 4% of immigrants entering the CPC are infected with COVID-19, and 11% leave the facility infected. This infection rate changes based on relative improvements to aerosol risk due to investments in ventilation and facility capacity, as well as reduction in exposure time (increasing processing speed). We additionally implemented the canonical SEIR equations within the Migration Process model to provide a basis for validation for the ABM model across the range of parameters.

Limited information was known about the CPC facilities when developing the CFD model (Figure 8). Several assumptions needed to be made to perform the analysis, including the following: 1) approximations to model geometry – only general dimensions were provided (height, length), so published photographs were used to approximate the model dimensions for both the building, partitions, and ducting (inlets, outlets, etc.); 2) no furniture or people were included in the model to decrease complexity; 3) doors to outside the building are kept closed.

To show the SEIR model's s ability to measure impact to local communities, we assume for demonstrative purposes that immigrants, after release, travel to Houston, Miami, El Paso, Los Angeles, Dallas, and Atlanta.

3.2.2. Costs and implementation challenges of NPIs

Each NPI we consider differs in efficacy and is subject to specific implementation challenges; from permitting, to construction, maintenance, or headcount. We considered NPI "portfolios" along three dimensions: changes in facility capacity, processing time, and HVAC upgrades. Cost estimates for facility construction were available through open contract databases usaspending, while the cost of HVAC upgrades was estimated by subject matter experts.

The main drivers of cost for the NPIs considered include:

- Tent space: construction cost, material cost, time
- Time in CPC: increase labour costs, increased headcount, improved logistics/communication systems
- Ventilation: equipment cost, installation

3.3. Scenarios and results

CFD analysis resulted in the quantification of airflow (Figure 8) being distributed to each partition area, which was the partial fraction of the overall 27,000 cu. ft. per min (CFM) from the facility's engineering specifications. The specified airflow was then compared with the CFD analysis of partition doors open and resulted in improvements between 1% up to 11.4% depending on the partition area. Some areas within the facility showed a decrease in airflow by 5.8% with the partition doors opened due to the HVAC flows becoming more evenly distributed. We selected a medial sample partition area that had an 8% improvement in airflow with 2,194 CFM increasing to 3,148 CFM with the doors open.

The resulting CFD baseline airflows of the selected tent partition (2,194 CFM) were then used by the AR model along with the tradespace parameters of number of tent structures, increasing or decreasing airflows, population density inside the tent, and wearing of masks or not (Figure 9). The most effective strategy at reducing aerosol risk is to reduce the population density by increasing the number of tent

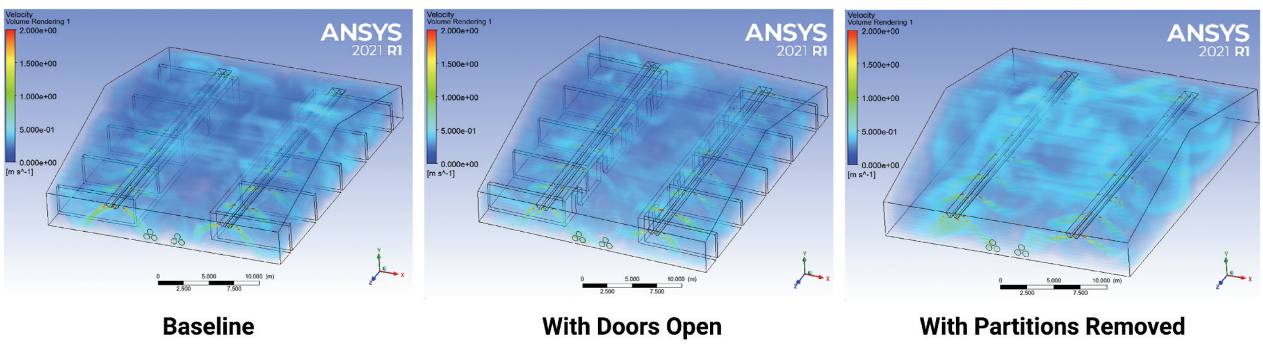

Figure 8. Velocity [m/s] distribution of the three investigated cases (L: doors closed [baseline], M: with the doors open, R: with the partitions fully removed).

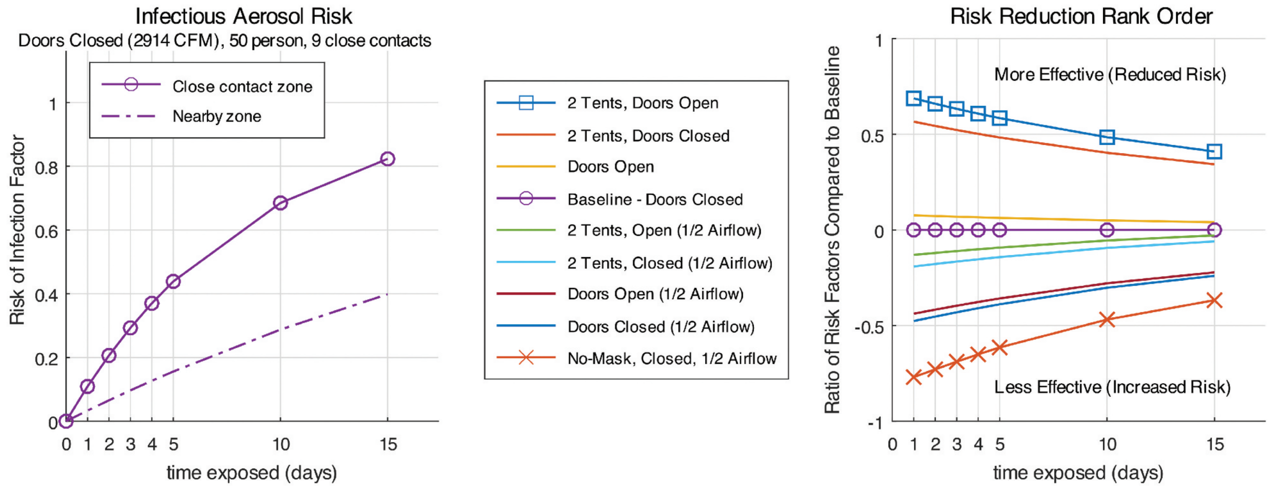

Figure 9. Infectious aerosol risk over time for close contacts and nearby people (i.e., In the same room) (left). The risk factor from each mitigation scenario is compared to the baseline condition (Figure 6) using the ratio quotient and then ordered by effectiveness (right). 2 tents with all doors open is the most effective, while reduced airflow and without face masks is the worst case condition. The effectiveness of all airflow configurations converge over time because the air space is eventually saturated infectious aerosols with the assumption of relatively stationary people.

50 persons/partition → **Increasing # Tents** → **25 persons/partition**

% Infected w/in Facility (50 persons/partition)

	10 Days	5 Days	1 Day
Doors Closed (1457 CFM)	31.14%	11.55%	4.70%
Doors Open (1574 CFM)	28.02%	10.52%	4.64%
Doors Closed (2194 CFM)	10.44%	6.48%	4.34%
Doors Open (3148 CFM)	9.69%	6.16%	4.25%

% Infected w/in Facility (25 persons/partition)

	10 Days	5 Days	1 Day
Doors Closed (1457 CFM)	14.39%	7.28%	4.37%
Doors Open (1574 CFM)	12.92%	7.06%	4.36%
Doors Closed (2194 CFM)	6.78%	5.26%	4.10%
Doors Open (3148 CFM)	6.35%	5.12%	4.10%

Figure 10. Heatmaps show the percent of immigrants infected within CPC based on 1) the number of immigrants per tent partition, 2) immigrant processing time (here assumed same for all agents-types), 3) doors louvered or sealed, and 4) HVAC level in CFM. Note (as indicated by color) that reducing the processing time to one day is the best defense against disease spread, followed by high ventilation, reducing partition capacity, and louvered doors (in that order). Baseline case corresponds to 50 ppl/part., 10 days, doors closed, 2194 CFM.

structures (68% improvement) at day 1, compared to the worst case of no-mask requirements and reduced airflow which had a 77% reduction of effectiveness and significant increase in risk. The improvements shown in (Figure 9) are the inverse of the aerosol risk ratios $\frac{R_S}{R_B}$ which are used as a scenario multiplier of $\rho = 0.07$ as inputs to ABM and ultimately the SEIR model.

In order to translate between the ABM and SEIR we run the ABM in a Monte-Carlo mode for 32 simulations. These simulations run for 40 days, with statistical measurements taken for days 10–30. A warmup period of 10 days was necessary to reach steady state. With respect to using only 32 runs, all but one scenario exhibited a coefficient of variation (COV) less than 5% in the average number of infected migrants sent to the US after 32 runs. The single exception had a COV 5.4%, and this was considered reasonable for our demonstrative objectives. Increasing the number of runs to 100 reduces the maximum COV to 3.5% while requiring a significantly longer runtime.

These previously mentioned cost drivers were used as tradespace parameters in the ABM and SEIR models to show the effect of each on the per cent of immigrants infected at the CPC (Figure 10). Note that the overall results indicate that reducing the length of stay is the most effective NPI at reducing the spread of COVID-19 infection within the CPC. At one-day processing time, the per cent of immigrants infected barely increases from the 4% incoming, however, in the worst case (10-day, low airflow, high density) the CPC processing results in a 6X multiplier to the per cent infected. Building two new tents to reduce the population density to 25 persons per partition achieves a $\approx$ 50% reduction from worst case, while adding new ventilation and louvred doors achieves a $\approx$ 60% reduction from worst case.

Immigrant processing time is clearly the largest contributor to disease spread within the facility, and minimising the immigrant processing time should be the primary focus. However, reducing immigrant processing time is the most elusive NPI strategy we considered because it is not a one-time investment into fixed physical infrastructure. Reducing processing time requires increasing in headcount and

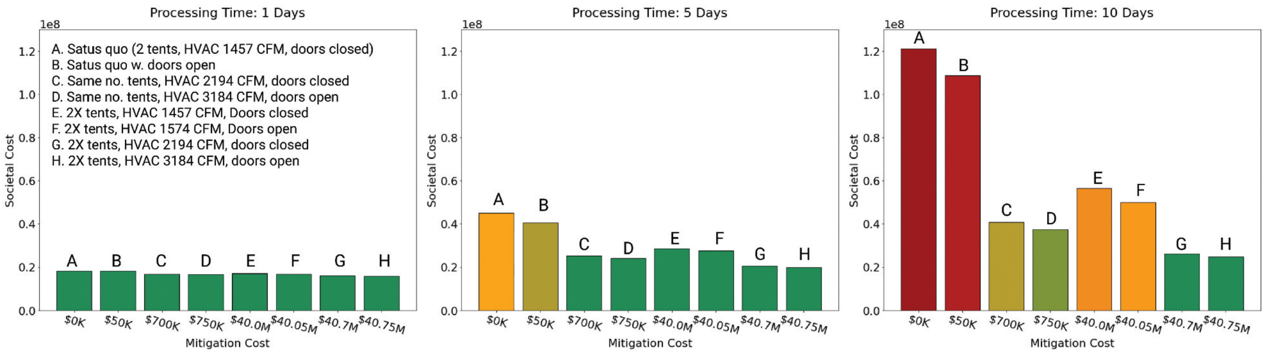

Figure 11. Simulation runs grouped by immigrant processing time with plots showing the relationship between investment in disease mitigation infrastructure and downstream societal cost. The cost of constructing additional tents (~ $40M) is orders of magnitude above the cost of other NPIs (louvered doors ~ $50K, HVAC ~ $700K).

streamlining facility processes, which far exceeds the scope of this effort. For this reason, we segment the societal cost results by immigrant processing time to compare the effects of the remaining NPIs at different processing speeds.

Figure 11 showcases the societal cost over 6 months of infections leaving the facility by investment in louvred doors, HVAC upgrades, and facility size. When a surge in migration results in a processing-speed reduction, ventilation and facility capacity become critical pieces of disease mitigation strategy.

4. Discussion

4.1. Theory of multiscale and multi-paradigm model composition

The composition of a multiscale and multi-paradigm model work must ensure alignment between sub-models: conceptually, theory, methods, assumptions, and constraints. For example, CFD and AR follow fluid dynamics theory and science but must also accommodate non-linear complex particle diffusion related to human emissions and movement patterns. ABM uses an entirely different set of dynamics where the non-homogeneous agents interact with one-another to emulate human movement yet follow a set of programmed constraints that model real-life parameters of interest. The SEIR compartmental model is based on the statistical dynamics of larger population (assuming homogeneity), but alone does not have the fidelity to estimate within small population environments where the leading risk factor is based on fluid dynamics. Additional consideration must be placed on the appropriateness of composing such a multiscale model and investigate the compatibility of assumptions and scale between each sub-model. Finally, the challenge of ensuring mutually exclusive parameters between models so that the correlation of covariates between models is minimised despite the multiple paradigms.

The first critical question to answer is on the appropriateness of composing the model in this work; without such an evaluation the research would be limited to a hypothetical computational domain that may not have a basis in a real-world problem. To consider the appropriateness, we use a causal factor tree analysis approach which qualitatively evaluates the effect or impact of each factor in the composite model. If the factor could have a significant effect on downstream models (e.g., physics, human contact, etc.), then it was considered important. In reverse order, the first element within the hybrid model to evaluate is the SEIR model which has largely been used by the epidemiology community since the early 20th century to track disease spread based on population statistics (Kermack & McKendrick, 1927; Ross, 1916). Yet the SEIR model is based on the premise that disease spreads from interaction between people in their local environments. ABM helps to quantify these interactions. The second pivotal dependency is on the quality and type of the interaction and the physical mechanism of disease spread such as airborne or fomite transmission. For COVID-19, it has been formally established that aerosolized viral particles are the primary transmission mechanisms (Morawska & Milton, 2020). Airborne propagation subsequently has dependencies on contagion emissions, airflow patterns, and inhalation or reductions from respiratory protection. All of these low-level factors are captured by the CFD and AR models. Conclusively, the qualitative evaluation of underlying factors using causal trees establishes that all four models can appropriately be composed.

Next, we evaluate the compatibility between models considering each paradigm, their underlying dynamics, assumptions, and a comparison of time domains. There are four interfaces between between the CFD, AR, ABM, SEIR models and the final SC calculation as numbered in Figure 2. The CFD model provides the air velocity and airflow rates within the enclosed space which are the primary determinants of the aerosol dispersion pattern and risk zones within the AR model. Both CFD and AR are bounded by physics laws in the field of fluid dynamics and are inherently considered the same paradigm with the same underlying assumption of constant airflow for the given analysis period. Likewise, CFD and AR share the same time domain of metres per second (air velocities) and airflow rates per minute.

The interface between AR and ABM is particularly interesting for two reasons: 1) it is an interface between two theoretical paradigms, and 2) different observational perspectives. The paradigm of aerosols and the laws of physics are very different than probabilistic interactions between people (agents). However, they both have a common basis: risk of infectious aerosol exposure. The key difference is that ABM allocates transmission events from the perspective of the infected agents, known as emitters, and probability of interacting with susceptible people. In contrast, the AR model provides a relative risk from the perspective of susceptible individuals and their exposure to infectious aerosols given environmental conditions of airflow patterns and the geometry of the enclosed area.

With regard to time domain, AR and ABM are also well aligned and use the common intersection of the first day for determining the initial risk. AR initially uses units of minutes based on aerosol propagation speeds from our prior field experiments (Edwards et al., 2020) but then uses days to account for overall accumulation of infectious particles in the contained environment and the resulting risk calculation. While the AR model provides a calculation for multiple days so that the relative effectiveness of aerosol mitigation methods (e.g., ventilation, filtration, etc.) can be compared over a longer period of time, ABM only leverages the AR risk factors from the first day as a baseline multiplier for R_0.

One potential issue that arises for any given time epoch in the composite model are the parameters of mask usage and mask filtration efficiency for both AR and ABM. In order to ensure mutual exclusion of variables and minimise double counting or duplicative effect, mask efficiency is used in AR to calculate the infectious aerosol dispersion pattern and propagation regions of higher particle concentrations. In contrast, ABM uses mask filtration efficiency and the percentile of population wearing of masks to determine the quality of interaction and degrade the transmission probability which is more representative of real environments such as (Lindsley et al., 2021).

The total number of infected and susceptible people are also common to both AR and ABM. AR uses the density of people along with airflow to determine the risk of exposure to an infectious aerosol cloud's propagation from talking, sneezing, or coughing considering the distance to susceptible people that are relatively stationary. Yet ABM uses these numbers to calculate probability of interaction. The risk probabilities from agent interaction are starkly different than aerosol dispersion distances and concentrations.

A final evaluation of multi-scale model compatibility considers the scale between each model also provides validity of composing this multiscale and multi-paradigm hybrid model. The CFD and AR interface use the same physical units and scale, however the scale between AR to ABM interface and that of ABM to SEIR are not as apparent. The AR model outputs a dimensionless multiplier of infection risk relative to the baseline airflow and density of people (e.g., 2,194 CFM and 50 persons/partition) in the local environment. Since clinical study data using the AR model does not exist it would not be appropriate to call it a probability, yet the resulting risk factor can be used in a similar mathematical construct when combining two probabilities and can be used to scale the rate of infection in the ABM if the AR model can meet the same assumption of homogeneity (for a mathematical basis see Appendix B).

4.2. Validation

Because a composite infectious disease model like this does not exist in published work, validation of the model is performed by two methods. First, each model within the overall composition is validated using best practices in their specific domains. Second, the overall composite model outcome data using baseline conditions (status quo described in Figure 6) is compared to historical COVID-19 transmission data to ensure it is within a margin of error.

For CFD analysis (NASA, 2021b), the most accurate validation method is to perform physical testing and compare to the computational results. Since physical testing was outside the scope of this investigation, steps were taken within the CFD process to ensure converged results. For example, in a steady state simulation, the model should have converged such that the total airflow into the system is acceptably close to the total airflow out. Input and output flow rates were compared for each of the different simulations to confirm such steady state behaviour. Additionally, a mesh convergence study (NASA, 2021a) was performed to ensure that the mesh used was sufficiently dense for representing the relevant aspects of the airflow.

Since the AR model is an emergent method used for comparative analysis of aerosol risk, and specific related human studies do not exist, standard methods such as cross-validation or fit of data cannot be used. Using the validated 1978 Wells-Riley formula as the basis, we break apart the problem into near field (close contact) and far field (same room) calculations. We use an approximate dispersion distance and peak concentration value derived from our prior empirical work on aerosol dispersion (Edwards et al., 2020, 2021) and based on the airflow from CFD. These two factors determine the quanta and viral emissions used in the Well-Riley equation for the close contact zone. A similar calculation is performed for the remaining areas in the room partition (i.e., nearby zone), but with a lower concentration and therefore lower quanta and emissions, also based on our prior aerosol dispersion work. Since the resultants of both the close contact and nearby area cannot yet be validated with human studies, it becomes a risk factor rather than a probability. Therefore, we use the ratio of the resultants from various mitigations to that of status quo to generate the rank order for comparison. The final data as shown in Figure 9 is then qualitatively validated based on a large body of infectious aerosol research to ensure the improvements or worsened effects were appropriately ordered and with a relative scale that is comparable to prior work (Edwards et al., 2021).

In this use case, the ABM/process model can be reduced to a heterogeneous queue with disease transmission. There was minimal historical data to fully validate the ABM model; however, we perform a limited validation using this data. This data included the arrival rate of immigrants at the border that were sent to the CPC, the average processing times for each demographic (UACs, FMUAs, SAs), and the number of people in the facility for each demographic. Arrival rates and processing times were used to verify that migrant outflows match CBP data for March 2021.

Additionally, the infection rate was tuned to reproduce the infection data under the baseline conditions (status quo described in Figure 6). Agency data showed 4% of immigrants entering the facility were infected with COVID-19, which grew within the facility to 11% infected leaving the facility. Once this was completed, the infection rate of the ABM model was then adjusted to fit the percent infected exiting the facility, and yielded coefficient of variation in the steady-state values of existing infections of less than 0.011.

The SEIR-based model's logic was reviewed by medical experts including physicians, epidemiologists, and microbiologists within the author's organisation, and sensitivity analyses were used to test model behaviours. In order to simulate COVID-19 spread within a given MSA, the SEIR-based model fits multipliers for local contact rate, mask usage, and disease severity to historical COVID-19 deaths (*US COVID-19 cases and deaths by State*, 2021). The results included this work were subsequently regenerated in September 2021, where the model fit to COVID-19 death data from February 2020-April 2021 (see Figure 12).

Fatalities are a more reliable indicator of epidemic progression than reported cases, especially with regard to SARS-CoV-2, as reported cases only include cases confirmed by testing (which excludes many asymptomatic and symptomatic cases). Yet fitting to this dataset does have a significant issue to consider: it includes the effect of the phenomenon we intend to model. If we injected a flow of infected immigrants into an MSA exactly equal to the empirical flow of infected immigrants because our SEIR model is fit to a timeseries of deaths, we would in effect be doubling the flow of infected immigrants. However, attempting to accurately extract the existing flow of immigrants would involve data out of the scope of this effort, while the ranked order of alternatives is still preserved with its presence. SC is not validated since it is a simple cost multiplier applied to the SEIR outcome results based on reported values (Hackett, 2020; U.S. Department of Transportation, 2021).

4.3. Generalization

This work was produced for a highly specified purpose and applied context; however, the composite model framework can be applied to the indoor spaces of any campus-like environment with relatively homogeneous interaction networks for infectious disease or similar problems. We believe the considerations and discussion around connecting the various physical domain models (CFD, AR) to ABM and SEIR compartmental and probabilistic models can be generally applied to other real-world problem sets. Researchers would need to select the appropriate physical models

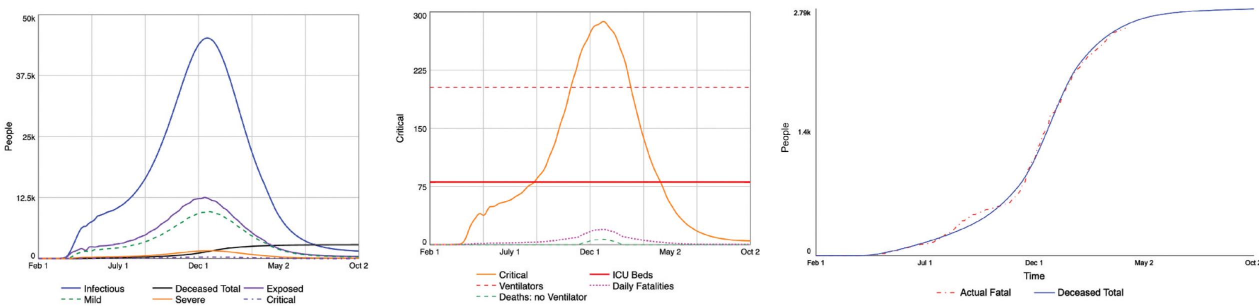

Figure 12. Sample output from a SEIR run in El Paso, TX, a primary destination for immigrants leaving processing centers in the Rio Grande Valley. Plots show the time course of population in various disease states (left), hospitalized population and ventilator capacity (center), and model deaths versus USA facts reported deaths (right).

and probabilistic models while tailoring them to the problem set while considering what inputs and outputs have significant influence on the downstream model. There is much research to explore the nuances of multi-scale, multi-paradigm models for additional research problem sets but we hope our current work can help inform the future work.

As discussed in the introduction, we can leverage institutional materials (e.g., facility blueprints, schedules for facility operations, databases, enterprise resource planners, etc.) to achieve verifiable models. Combining this information with qualitative behavioural data from SMEs allows us to quickly approach and accurate computational model of day-to-day campus operations.

4.4. Challenges of real-time modeling

This research effort began during a surge in COVID-19 cases in the US, Mexico, and at the border. Both the pandemic and the situation at the border were not only non-stationary systems but were quickly evolving. The consequence of trying to study such a class of problems is constant remodelling to factor in relevant real-world developments (Delta and Omicron variants, Haitian border crisis, etc.). To meet this challenge, models should be properly modularised and situations/scenarios should be parametrised. These considerations play an important role in the ability to use any such computational tools for decision-making.

4.5. Decision-making

This project, and most applied research works, intend to inform some component of real-world decision-making. The most critical of the challenges posed by "real-time modelling" is the lack of time (and often data) to properly validate models. However, the validation and data requirements to assess model accuracy far exceed the validation requirements of predicted lower and upper bounds of real-world outcomes or a ranked order of alternatives, which still greatly inform decision-making. We must approach model output with a high degree of scepticism but realise that unvalidated models with tractable logic and proper constraints provide a stronger foundation for decision-making than mental models.

Acknowledgments

We would like to acknowledge the support of the MITRE Center for Securing the Homeland (CSH), who manages Homeland Security Systems Engineering and Development Institute, a Federally Funded Research & Development Center (FFRDC) for the DHS Enterprise (which includes Federal, State, Local, and Tribal Governments), as well as the National Cybersecurity FFRDC (NCF), the FFRDC for the NIST. We also thank the MITRE COVID-19 Analytics Team for their support and contributions.

This work was supported by independent research and development funding provided by the author's organisation, The MITRE Corporation.

Disclosure statement

No potential conflict of interest was reported by the author(s).

Data availability statement

The models used in this study are available to US national, state, and regional agencies as well as healthcare systems on request to the corresponding author.

References

Ansys 2021R1 (CADFEM) https://www.cadfem.net/en/cadfem-informs/newsroom/ansys-release/ansys-release-.html 2021

Aron, J. L., & Schwartz, I. B. (1984, October). Seasonality and period-doubling bifurcations in an epidemic model. *Journal of Theoretical Biology*, *110*(4), 665–679. https://doi.org/10.1016/S0022-5193(84)80150-2

Benjamin, D. K., & Zimmerman, K. (2021, June). *Final report for NC School Districts and charters in plan A: March 2021 through June 2021*. Tech. Rep. The ABC Science Collaborative.

Bhuvan, K., Shrestha, R., Leggat, P. A., Shankar, P. R., & Shrestha, S. (2021). Safety of air travel during the ongoing COVID-19 pandemic. *Travel Medicine and Infectious Disease*, *43*, 102103. https://doi.org/10.1016/j.tmaid.2021.102103

Chagla, Z., Hota, S., Khan, S., Mertz, D., Hospital, I., & Group, C. E. (2020, 08). Re: It is time to address airborne transmission of COVID-19. *Clinical Infectious Diseases*, *73*(11), e3981–e3982. https://doi.org/10.1093/cid/ciaa1118

Chen, P., Fan, W., Guo, X., & Siettos, C. (2021). A hybrid simulation model to study the impact of combined interventions on Ebola epidemic. *PLoS One*, *16*(7), e0254044. https://doi.org/10.1371/journal.pone.0254044

Cuevas, E. (2020). An agent-based model to evaluate the COVID-19 transmission risks in facilities. *Computers in Biology and Medicine*, *121*, 103827. https://doi.org/10.1016/j.compbiomed.2020.103827

De Visscher, A. (2020). The COVID-19 pandemic: Model-based evaluation of non-pharmaceutical interventions and prognoses. *Nonlinear Dynamics*, *101*(3), 1871–1887. https://doi.org/10.1007/s11071-020-05861-7

Drossinos, Y., Reid, J. P., Hugentobler, W., & Stilianakis, N. I. (2022). Challenges of integrating aerosol dynamics into SARS-CoV-2 transmission models. *Aerosol Science and Technology*, *56*(9), 777–784. Retrieved January 4, 2023 . https://doi.org/10.1080/02786826.2022.2102792

Edwards, N. (n.d.). *TRB TCRP Insight Event Air Quality in Transit Buses: Transit Airflow Verification Studies.*

Transit Cooperative Research Program (TCRP). https://www.nationalacademies.org/event/06-21-2022/trb-tcrp-insight-event-air-quality-in-transit-buses

Edwards, N. J., Widrick, R., Potember, R., & Gerschefske, M. (2020, December). Quantifying respiratory airborne particle dispersion control through improvised reusable masks: The physics of non-pharmaceutical interventions for reducing SARS-CoV-2 (COVID-19) air- borne transmission. *Journal of Nanotechnology and Nanomaterials*, *1*(3), 116–128. Pub- lisher: ScientificArchives.

Edwards, N. J., Widrick, R., Wilmes, J., Breisch, B., Gerschefske, M., Sullivan, J.,et al. (2021). Reducing COVID-19 airborne transmission risks on public transportation buses: An empirical study on aerosol dispersion and control. *Aerosol Science- Ence and Technology*, *55*, 0. https://doi.org/10.1080/02786826.2021.1966376

Hackett, M. (2020 November). The average cost of hospital care for COVID-19 ranges from $51,000 to $78,000 based on age. *Healthcare Finance News*. Retrieved October 7, 2021, from https://www.healthcarefinancenews.com/news/average-cost-hospital-care-covid-19-ranges-51000-78000-based-age

Hunter, E., MacNamee, B., & Kelleher, J. (2020). A hybrid agent-based and equation based model for the spread of infectious diseases. *Journal of Artificial Societies and Social Simulation*, *23*(4). https://doi.org/10.18564/jasss.4421

Kanno-Youngs, Z. (2021). *Biden Under Pressure Over 'Public health' Border Expulsions*. Retrieved 10-18, 2023, from https://www.nytimes.com/2021/05/24/us/politics/biden-border-immigrants.html

Karimzadeh, S., Bhopal, R., & Tien, H. N. (2021). Review of infective dose, routes of trans- mission and outcome of COVID-19 caused by the SARS-COV-2: Comparison with other respiratory viruses. In *Epidemiology & infection* 116 (Vol. 149). Cambridge University Press) doi:10.1017/S0950268821000790.

Kendall, D. G. (1956, January). Deterministic and stochastic epidemics in closed populations. *Proceedings of the Third Berkeley Symposium on Mathematical Statistics and Probability, Volume 4: Contributions to Biology and Problems of Health*, *3 4* (pp. 149–166). Publisher: University of California Press.

Kermack, W. O., & McKendrick, A. G. (1927, August). A contribution to the mathematical theory of epidemics. *Proceedings of the Royal Society of London: Series A, Containing Papers of a Mathematical and Physical Character*, *115*(772), 700–721. (Publisher: Royal Society).

Kerr, C. C., Stuart, R. M., Mistry, D., Abeysuriya, R. G., Rosenfeld, K., Hart, G. R., & others. (2021). Covasim: An agent-based model of COVID-19 dynamics and interventions. *PLoS Computational Biology*, *17*(7), e1009149. https://doi.org/10.1371/journal.pcbi.1009149

Kunwar, P., Markovichenko, O., Chyba, M., Mileyko, Y., Koniges, A., & Lee, T. (2021). A study of computational and conceptual complexities of compartment and agent based models, *arXiv Preprint arXiv 17*(3), 359. https://doi.org/10.3934/nhm.2022011

Lindsley, W. G., Blachere, F. M., Beezhold, D. H., Law, B. F., Derk, R. C., Hettick, J. M., et al. (2021). A comparison of performance metrics for cloth masks as source control devices for simulated cough and exhalation aerosols. *Aerosol Science and Technology*, *55*(10), 1–18. (Publisher: Taylor & Francis). https://doi.org/10.1080/02786826.2021.1933377

The MITRE Corporation. (2020). *Coronavirus (COVID-19) Non-Pharmaceutical Interventions Prototype Tool*. Retrieved. March 26, 2021, from https://exchange.iseesystems.com/public/stephanieglasser/covid-npi/index.html

Mittal, R., Meneveau, C., & Wu, W. (2020). A mathematical framework for estimating risk of airborne transmission of COVID-19 with application to face mask use and social distancing. *Physics of Fluids*, *32*(10), 101903. (Publisher: American Institute of Physics)

Morawska, L., & Milton, D. K. (2020, November). It is time to address airborne transmission of coronavirus disease 2019 (COVID-19). *Clinical Infectious Diseases*, *71*(9), 2311–2313. https://doi.org/10.1093/cid/ciaa939

NASA. (2021a). *Examining Spatial (Grid) Convergence*. Retrieved 10-18 2023, from https://www.grc.nasa.gov/WWW/wind/valid/tutorial/spatconv.html

NASA. (2021b). *Overview of Cfd Verification and Validation*. Retrieved 10-18, 2023, from https://www.grc.nasa.gov/www/wind/valid/tutorial/overview.html

Netz, R. R., & Eaton, W. A. (2020, October). Physics of virus transmission by speaking droplets. *Proceedings of the National Academy of Sciences*, *117*(41), 25209–25211. https://doi.org/10.1073/pnas.2011889117

Nguyen, L. K. N., Megiddo, I., Howick, S., & Struchiner, C. J. (2022). Hybrid simulation modelling of networks of heterogeneous care homes and the inter-facility spread of COVID-19 by sharing staff. *PLoS Computational Biology*, *18*(1), e1009780. https://doi.org/10.1371/journal.pcbi.1009780

Pan, M., Lednicky, J. A., & Wu, C.-Y. (2019). Collection, particle sizing and detec- tion of airborne viruses. *Journal of Applied Microbiology* [eprint], *127*(6), 1596–1611. https://sfamjournals.onlinelibrary.wiley.com/doi/pdf/10.1111/jam.14278)

Parhizkar, H., Van Den Wymelenberg, K. G., Haas, C. N., & Corsi, R. L. (2022). A quantitative risk estimation platform for indoor aerosol transmission of covid-19. *Risk Analysis*, *42*(9), 2075–2088. https://doi.org/10.1111/risa.13844

Ramajo, D. E., Corzo, S. (2022). Airborne transmission risk in urban buses: A compu- tational fluid dynamics study. *Aerosol and Air Quality Research*, *22*(8), 210334. https://doi.org/10.4209/aaqr.210334

Ramirez, D. W. E., Klinkhammer, M. D., & Rowland, L. C. (2021, July). COVID-19 trans- mission during transportation of 1st to 12th grade students: Experience of an Independent School in Virginia. *Journal of School Health*, *91*(9), 678–682. https://doi.org/10.1111/josh.13058

Riley, E. C., Murphy, G., & Riley, R. L. (1978). Airborne spread of measles in a suburban elementary school. *American Journal of Epidemiology*, *107*(5), 421–432. https://doi.org/10.1093/oxfordjournals.aje.a112560

Ross, R. (1916). An application of the theory of probabilities to the study of a priori path- ometry.—part i. *Proceedings of the Royal Society of London: Series A, Containing Papers of a Mathematical and Physical Character*, *92*(638), 204–230.

Rudnick, S. N., & Milton, D. K. (2003). Risk of indoor airborne infection transmission estimated from carbon dioxide concentration. *Indoor Air*, *13*(3), 237–245. https://doi.org/10.1034/j.1600-0668.2003.00189.x

Russonello, G. (2021). *What's Driving the Surge at the Southern Border?* Retrieved 10-18, 2023, from https://www.nytimes.com/2021/04/05/us/politics/biden-immigration-crisis.html

Sickbert-Bennett, E. E., Samet, J. M., Clapp, P. W., Chen, H., Berntsen, J., Zeman, K. L., et al. (2020, December). Filtration efficiency of hospital face mask alternatives available for use during the COVID-19 pandemic. *JAMA Internal Medicine*, *180*(12), 1607. https://doi.org/10.1001/jamainternmed.2020.4221

Sze to, G. N., Wan, M. P., Chao, C. Y. H., Wei, F., Yu, S. C. T., & Kwan, J. K. C. (2008). A methodology for estimating airborne virus exposures in indoor environments using the spatial distribution of expiratory aerosols and virus viability characteristics. *Indoor Air*, *18*(5), 425–438. https://doi.org/10.1111/j.1600-0668.2008.00544.x

Timothy, J. J., Holla, V., & Meschke, G. (2020). Multiscale dynamics of COVID-19 and model- based recommendations for 105 countries. *medRxiv* https://doi.org/10.1101/2020.06.05.20123547.

Tolk, A., Harper, A., & Mustafee, N. (2021, June). Hybrid models as transdisciplinary research enablers. *European Journal of Operational Research*, *291*(3), 1075–1090. https://doi.org/10.1016/j.ejor.2020.10.010

Us COVID-19 Cases and Deaths by State. (2021, November). https://usafacts.org/visualizations/coronavirus-covid-19-spread-map/

U.S. Department of Transportation. (2021, March). *Departmental Guidance on Valuation of a Statistical Life in Economic Analysis*. Retrieved October 7, 2021, from https://www.transportation.gov/office-policy/transportation-policy/revised-departmental-guidance-on-valuation-of-a-statistical-life-in-economic-analysis

Wildman, W. J., Diallo, S. Y., Hodulik, G., Page, A., Tolk, A., Gondal, N., & Xu, X. (2020). The artificial university: Decision support for universities in the COVID-19 era. *Complexity*, *2020*, 1–10. https://doi.org/10.1155/2020/5910209

Yarsky, P. (2021). Using a genetic algorithm to fit parameters of a COVID-19 seir model for us states. *Mathematics and Computers in Simulation*, *185*, 687–695. https://doi.org/10.1016/j.matcom.2021.01.022

Young, L.-S., Danial, Z., & Souza, M. O. (2021). Three pre-vaccine responses to covid-like epidemics. *PLOS One*, *16*(5), e0251349. https://doi.org/10.1371/journal.pone.0251349

Zhou, Y., Li, L., Ghasemi, Y., Kallagudde, R., Goyal, K., & Thakur, D. (2021). An agent-based model for simulating COVID-19 transmissions on university campus and its implications on mitigation interventions: A case study. *Information Discovery and Delivery*, *49*(3), 216–224. https://doi.org/10.1108/IDD-12-2020-0154

Appendix A. Detailed Description of Individual Models

Computational Fluid Dynamics Model

Computational Fluid Dynamics (CFD) uses numerical methods to simulate the fluid flow within a space, providing results on flow rate, particle trajectory, etc. In this case, CFD modelling was used to evaluate the airflow within the building in question, identifying potential areas of concern (low airflow) where COVID-19 transmission could be high. In addition, this analysis investigated how opening or closing the doors to the portioned rooms would affect airflow: an increase of the overall airflow rate to these spaces therefore decreases the risk of COVID-19 transmission (Parhizkar et al., 2022). The results of this analysis can be used to inform both short-term changes to facilities and design decisions for new buildings. To complete a CFD simulation, a computer aided design (CAD) model of the building and specifications about the airflow within that space are required. A CAD model was developed using Ansys 2021, R1 to represent this space, and Heating/Ventilation/Air Conditioning (HVAC) specifications provided by the facility were used to produce a fluid flow analysis. The CFD airflow rates and resulting air changes per hour (ACH) assist in the aerosol risk quantisation, however the airflow dynamics as shown in the CFD streamlines (see Figure 8) help gain significant understanding of infectious aerosol travel or accumulation in stagnant regions.

Inputs

- Dimensions and layout of facility (building size, ducting placement, etc.)
- HVAC system specifications (airflow into facility, given in cu. ft. per min (CFM))

Outputs

- Airflow streamlines – the general layout of airflow patterns throughout the building (velocity)
- Airflow rates – CFM of air going in or out of the partitioned areas due to effects of opening or closing partition
- Air changes per hour (ACH) in partition areas and overall facility

Key Assumptions Airflow occurs at a constant rate for the simulation run-time. Temperature and humidity effects on airflow were not analysed and were kept as constants. Temporal interruptions to airflow dynamics such as people movement or temporarily opening and closing doors were assumed to be static for comparative analysis between scenarios.

Important Notes Convergence is critical to producing an accurate CFD simulation. There are several factors that affect convergence, including mesh size, turbulence parameters, and number of iterations in the simulation. These factors were all considered when performing the final analysis.

Aerosol Risk Model

An aerosol risk model provides an estimate risk of exposure to airborne contagions or hazards (Mittal et al., 2020; Riley et al., 1978; Rudnick & Milton, 2003; Sze to et al., 2008). In the context of COVID-19 transmission, the model focuses on aerosols that are commonly defined as airborne particles that are 5 µm or less in size and are affected more by airflow and fluid dynamics than deposition from gravity (Pan et al., 2019). Since airborne infectious disease transmission is dependent on the loading human infectious dose (HID) into the respiratory tract, a measured quantity of contagions, and the exposure also strongly depends on nearby concentration(s) of the contagion, respiratory rates of the susceptible person, and the generation source of the contagion. This aerosol risk model primarily focuses on the movement and spread of the contagion through the air and includes effects from air exchange, and exposure regions based on infectious aerosol emitters and susceptible people. A broadly used aerosol risk model, Riley et al. (1978) (Riley et al., 1978), and many of the derivative models account for the major factors, however, they primarily consider a well-mixed environment and do not account the fluid dynamics near an infected or susceptible person. The aerosol risk model introduced in this work, built with GNU Octave version 6.2.0, uses the Wells-Riley model as a basis but adds the fluid dynamics and accounts for the aerosol dispersion pattern close to an infectious source, in the nearby vicinity or same room, the effects of wearing face masks or applying air filtration, and is derived from empirical observations of prior aerosol dispersion experimentation (Edwards et al., 2020, 2021).

Close contact of susceptible people to infected is defined by regions of higher infectious aerosol concentration after a dispersion event such as talking, coughing, or sneezing. In many cases, close contact is within a one-metre distance from an infected person (Figure 3) based on our empirical experimentation on aerosol dispersion (Edwards et al., 2020, 2021) and is informed by the air velocity analysis from CFD simulation. In other conditions with poor airflow, the peak concentration aerosol cloud can rapidly spread to 4 metres or more. Viral emissions or inhalation is reduced by the mask efficiency, although mask wearing compliance is not modelled in the aerosol risk model. The viral emissions increase with more infected people in the area. The Aerosol Risk (AR) model is run with [t] = [minutes] to calibrate the model, however the data is presented in days.

Infectious aerosol risk factor $\frac{R_S}{R_B}$, where R_S is the AR risk factor of the scenario and R_B be the AR risk factor of the baseline case. This ratio is used as a relative risk multiplier of the basic infection reproduction number, R_0, and scales the rate of infection in the Agent-Based Model (ABM).

We ran our ABM model with SME given nominal parameter values (initial infection rate of 4%) and fit ρ to .07 to predict the SME-value ($\approx$ 10%) for steady state infection rate of children arriving at HHS. We associated this ρ value to correspond to the AR risk of infection on day 1 of the AR's nominal case with doors closed and moderate airflow at 2914 CFM. We then adjusted the ρ value used in the ABM for the other AR cases by the aerosol risk factor. We are assuming the ratio of the risks is constant in time for the larger CFM cases (2914, 3148 CFM) where there is more of a steady state on infectious aerosol removal. However, in the low airflow cases (1457, 1574 CFM), the increase of residual infectious aerosols also increases the risk of exposure for people within the vicinity. The resulting infections function as a lower bound for the true number of infections, and remain consistent in the rank order of alternatives. More details on the use and interaction between AR and ABM using the risk multiplier are further described in Section 4.1 on the theory.

Inputs

- Room dimensions (*length, width, height*)
- Airflow rate in cu.ft.^{3}/minute (CFM)
- Air velocity for given room – estimated from CFD airflow streamlines and patterns
- No. Susceptible in close contact (3 ft. x 3 ft. grid) surrounding infected person

- No. Susceptible in room or area with same airflow region
- Height of infected person's head (aerosol emission spread pattern)
- Virion emission rate (3,000 virions per minute x mask filtration reduction) (Netz & Eaton, 2020))
- Estimated viral load to cause infection. Conservative value of 1000 viral copies was used based on (Karimzadeh et al., 2021)
- Volume of human respirations m^3per unit of time. Ave human $\sim 0.000566\ m^3$/min or 0.566 L/min.
- Mask filtration efficiency both for source filtration and personal protection (PPE). Mask filtration efficiency average of 38.1% was used for this analysis (Sickbert-Bennett et al., 2020)
- HVAC filtration efficiency. Baseline analysis performed without filtration in use-case facility.
- Unit of time (minutes or hours)

Outputs

- Infectious aerosol risk factor $\frac{R_S}{R_B}$, where R_S is the AR risk factor of the scenario and R_B be the AR risk factor of the baseline case. This ratio is used as a relative risk multiplier of the basic infection reproduction number, R_0, and scales the rate of infection in the ABM. Details on the use and interaction between AR and ABM using the risk multiplier are further described in Section 4.1 on the theory.
- Relative rank order on effectiveness of scenario environment variables (airflow, mask efficiency, etc.) and aids in mitigation decisions.

Key Assumptions Airflow occurs at a constant rate for the baseline analysis time period. This model also assumes that people are relatively stationary and generally stay within the same area or vicinity. For the US border immigrant processing use-case, immigrants stay within the assigned tent area and nearby their family units although they are allowed to move freely to and from their sleeping or waiting areas to the bathrooms. Therefore, the primary infectious aerosol exposure over a cumulative time would occur within their assigned tent area. Gross movement of people related to the acute infectious aerosol exposure or exposure to a tent area with high accumulation overtime is captured by the ABM.

Important Notes Close contact of susceptible people to infected is defined by regions of higher infectious aerosol concentration after a dispersion event such as talking, coughing, or sneezing. In many cases, close contact is within a one-metre distance from an infected person (Figure 3) based on our empirical experimentation on aerosol dispersion (Edwards et al., 2020, 2021) and is informed by the air velocity analysis from CFD simulation. In other conditions with poor airflow, the peak concentration aerosol cloud can rapidly spread to 4 metres or more. Viral emissions or inhalation is reduced by the mask efficiency, although mask wearing compliance is not modelled in the aerosol risk model. The viral emissions increase with more infected people in the area. The AR model is run with [t] = [minutes] to calibrate the model; however, the data is presented in days.

Agent-Based Infection Model

Agent-based modelling focuses on the individual components of a system as opposed to the homogeneous groups of compartmental models. We define behaviour for the components (agents) but study the emergent dynamics of the system. The flexibility of agent-based modelling allows us to implement facility operations to an arbitrary level of detail and simulate the infection process within the facility. In this model, the processing of different kinds of agents through a multistage process is much simpler than the homogenous assumptions necessary in the compartmental (SEIR) modelling approach.

This flexibility allows for the modelling of operational changes without having to change the underlying architecture of the model. This can be particularly useful in the context of a rapidly evolving situation like the COVID-19 pandemic, where new interventions and changes to operating procedures may be implemented frequently. With an agent-based model, it is possible to easily incorporate these changes into the simulation, providing a more accurate representation of the system and allowing for the evaluation of the potential impact of the changes. In our implementation and use case, the processing of different classes of agents through a multistage process is much preferred due to the significant compartment populations and homogenous assumptions necessary in a System Dynamics/SEIR modelling approach.

The agent-based model discussed here-in is a combination of an infection model and the model of the US southern border migration process (discussed in Section 3) implemented in AnyLogic version 8.6. Agents in the model represent individuals, each of which can be in one of six disease states (laid out in Figure 4): susceptible, incubating, infectious (either asymptomatic or symptomatic), recovered, dead, or immune and simultaneously 10 location states: At border, Holding[agent-type], Mexico, Health and Human Services (HHS), Immigration and Customs Enforcement (ICE), Non-Governmental Organisations (NGO), and within the US. The model tracks the movement of these agents through different areas of the facility (see process model in Figure 4) and simulates the spread of the disease as infected agents come into contact with others. The rate of infection is determined by several factors, including the transmissibility of the disease, the presence and effectiveness of masks, the vaccination status of the agents and the number of infected agents in a given agent's location.

The ABM outputs the number of new infections over time, which becomes an input into SEIR. Compartmental epidemic models are the mean field approximations of their agent-based equivalents under the assumption of homogeneity (Kunwar et al., 2021).

Inputs

- Immigrant arrival rate
- Per cent of population for each agent-type
- Processing rate each agent-type (Family Units: FMUAs, Single Adults: SAs, Unaccompanied Children: UACs)
- Population demographics (Age, Health Status)
- Disease characteristics (R_0, rate of infection)
- Time distribution for each disease state
- Per cent of SA sent back (Title 42)

Agent Behavior

- Agents arrive at the facility and move to a closed room within the facility
- Infectious agents randomly select from collocated susceptible agents (weighted draw based on mask usage, time in tent, and vaccination status)

- Once infected, agent transition through states according to delays (infectious to recovered, recovered to susceptible, immune to susceptible) and probabilities (incubating to asymptomatic/symptomatic, symptomatic to dead)

Outputs

- Number of new infections leaving facility per day allowed into the US

Key Assumptions Per cent initially infected and susceptible, rate of new infections, R_0, masking effectiveness and probability of wearing, time between exposed and symptomatic/asymptomatic state, symptomatic/asymptomatic duration. Note that the model assumes that agents can only die from the "Infectious Symptomatic" state; asymptomatic agents would eventually become symptomatic (such as shortness of breath) before death.

SEIR-Based Infection Model

Compartmental models such as Susceptible–Infected – Recovered (SIR) models have long been used in epidemiology to understand the high-level system dynamics of disease transmission within a population (Kendall, 1956; Kermack & McKendrick, 1927; Ross, 1916). SIR models can be fit to data and used to gauge the magnitude and timescale of the epidemic, as well as to understand the consequences of control decisions (Yarsky, 2021; Young et al., 2021). The system dynamics transmission model (SEIR) used in this body of work was derived from (Aron & Schwartz, 1984) and built on a SEIR framework which accounts for the long incubation period observed during the onset of COVID-19 with potential exposures (E) of susceptible people (The MITRE Corporation, 2020). The SEIR-based infection model used in this work (diagram in Figure 5) combines state and local Non-Pharmaceutical Interventions (NPIs), behavioural data, public/private health infrastructure, and empirical findings for the risk of hospitalisation and death, to produce a high-fidelity reconstruction of the epidemic. It contains sub-models for vaccination (according to a prescribed schedule), waning immunity/reinfection, and the rise of new variants. The core of our SEIR implementation is a data structure arrayed by age groups, with each age group having corresponding values for population size, likelihood of hospitalisation, likelihood of becoming critical, and likelihood of death. Additionally, the incubating, infectious, and recovered compartments are also arrayed by virus strain, with a disease severity for each strain. Infection risk is broken down into cohabitant versus social infectivity. The model also includes a blood plasma donation and administration module, as well as a vaccine production and administration module. For each city or metropolitan area, the model includes data on population size, the number of initial infections, the number of hospital beds and intensive care unit (ICU) beds per 1,000 people, and the number of ventilators per 10,000 people. The model was built using Stella Architect v2.1.3, and uses the included optimisation suite to fit disease severity to reported deaths for the respective location. The SEIR model simulates the pandemic trajectory in cities, metropolitan statistical areas (MSAs), subject to the flow of infected immigrants.

Inputs

- Initial state of system (percentage of the population susceptible, incubating, infectious, and recovered), generally assumed to be near the disease-free equilibrium (very small level of infection).
- Basic reproduction number, extracted from model fit
- Average number of contacts per person per unit time
- Number of new infections leaving facility per day allowed into the US

Outputs

- Number of infections, hospitalisations, recoveries, deaths

Key Assumptions Homogeneous network structure; exponential distribution of recovery time; contacts per person over time

Societal Cost Model

From the composite model outputs, we then calculate the additional hospitalisations and deaths from the increased number of infections. For purposes of comparison, the excess hospitalisations and deaths are quantified according to FAIR Health's analysis (Hackett, 2020) ~ \$65,000 per COVID-19 hospitalisation and US Department of Transportation using ~ \$10,000,000 as the statistical value of life (U.S. Department of Transportation, 2021). We use these costs to represent an NPI portfolio as (investment cost, societal cost/savings) to provide a quantitative decision trade-space on which NPIs should be implemented on-site.

Inputs

- Excess hospitalisations and deaths from SEIR model across MSAs

Outputs

- Cost representing excess treatments and loss of life resulting from a given NPI portfolio.

Key Assumptions \$65,000 per COVID-19 hospitalisation, \$10,000,000 statistical value of life.

Appendix B. Multi-scale Comparison Between Aerosol Risk and Agent Based Models

The parameter ρ in the ABM is the number of new infections per emitter per day, or more formally:

$$\rho = \mathbb{E}[\text{new infections per emitter perday}] = \frac{\sum_{i=1}^{N_p} P_i(\tau)}{N_{e,p}} \tag{B1}$$

where N_p is the number of agents in the room, $N_{e,p}$ is the number of emitters in the room, τ is the amount of time agent$_i$ has been in the room with an emitter, and $P_i(\tau)$ is the probability that agent$_i$ gets infected.

If we let R_S be the AR risk factor of the scenario and R_B be the AR risk factor of the baseline case; in both cases the linear dependence on P means that:

$$\frac{R_S}{R_B} \cdot \rho = \frac{\sum_{i=1}^{N_p} \frac{R_S}{R_B} \cdot P_i(\tau)}{N_{e,p}}, \tag{B2}$$

and that using the AR output as a relative risk multiplier to ρ in the ABM only imposes the assumption of homogeneous relative improvements for all agents. Due to the movement of people within the partition, bathroom, etc., the assumption of homogeneity for this risk factor is reasonable.